



1 Estimating Parameters in a Sea Ice Model using an Ensemble Kalman Filter

2 Yong-Fei Zhang^{1, 2*}, Cecilia M. Bitz¹, Jeffrey L. Anderson³, Nancy S. Collins³, Timothy J.
3 Hoar³, Kevin D. Raeder³, and Edward Blanchard-Wrigglesworth¹

4 ¹Department of Atmospheric Sciences, University of Washington, Seattle, Washington, USA.

5 ²Now at Program in Atmospheric and Oceanic Sciences, Princeton University, Princeton, New Jersey,
6 USA.

7 ³IMAGe, CISL, National Center for Atmospheric Research, Boulder, Colorado, USA.

12
13 Corresponding Author:

14 *Yong-Fei Zhang

15 Department of Atmospheric Sciences

16 Princeton University

17 4000 15th Ave NE

18 Seattle, WA 98195

19 USA

20 Phone: 1-512-298-9567

21 Email: yfzhang.nju@gmail.com

23 Key points:

- 24 • Parameter estimation using an ensemble filter is done in a sea-ice model.
- 25 • Parameters are improved during the data assimilation period.
- 26 • Large improvements in model states are seen in the forecast period.



30 Abstract

31 Uncertain or inaccurate parameters in sea ice models influence seasonal predictions and
32 climate change projections in terms of both mean and trend. We explore the feasibility and
33 benefits of applying an Ensemble Kalman filter (EnKF) to estimate parameters in the Los
34 Alamos sea ice model (CICE). Parameter estimation (PE) is applied to the highly influential dry
35 snow grain radius and combined with state estimation in a series of perfect model observing
36 system simulation experiments (OSSEs). Allowing the parameter to vary in space improves
37 performance along the sea ice edge compared to requiring the parameter to be uniform
38 everywhere. We compare experiments with both PE and state estimation to experiments with
39 only the latter and found that the benefits of PE mostly occur after the DA period, when no
40 observations are available to assimilate (i.e., the forecast period), which suggests PE's relevance
41 for improving seasonal predictions of Arctic sea ice.

42

43

44

45

46

47

48

49

50

51

52



53 1. Introduction

54 Arctic sea ice has undergone rapid decline in recent decades in all seasons (e.g., *Stroeve et al.*,
55 2012; *Serreze and Stroeve*, 2015). The frequent large deviations of Arctic sea ice cover from its
56 climatology and the impact of sea ice cover on the overlying atmosphere and on ocean-
57 atmosphere fluxes motivates including an active sea ice component in seasonal to sub-seasonal
58 (S2S) weather forecasts (*Vitart et al.*, 2015). The persistence and reemergence of sea ice
59 thickness (SIT) and SST anomalies are major sources of predictability for Arctic sea ice extent
60 (*Blanchard-Wrigglesworth et al.*, 2011). Previous studies have demonstrated the importance of
61 accurate initial conditions, especially SIT, in predicting Arctic sea ice extent (*Day et al.*, 2014).
62 Hence studies applying data assimilation (DA) techniques to fuse observations with model
63 simulations are growing (e.g., *Lisæter et al.*, 2003; *Chen et al.*, 2017; *Massonnet et al.*, 2015),
64 most of which are focused on improving model states only, not the parameters in the sea ice
65 component.

66 Sea ice models, like other components of earth system models, can suffer large uncertainties
67 originating from uncertain parameters. The widely used Los Alamos sea ice model version 5
68 (CICE5), given its various complex schemes, has numerous uncertain parameters, such as in the
69 delta-Eddington shortwave radiation scheme (*Briegleb and Light*, 2007). The default values of
70 these parameters are usually chosen based on point-scale measurements that are taken on multi-
71 year sea ice (*Light et al.*, 2008). *Urrego-Blanco et al.* (2015) conducted an uncertainty
72 quantification study of CICE5 and ranked the parameters based on the sensitivities of model
73 predictions to a list of parameters. This work provides guidance on which parameters could be
74 estimated using an objective method and during which seasons. Their findings suggest that the
75 estimates of the Arctic sea ice area and extent are especially sensitive to certain parameters (e.g.,



76 snow conductivity and snow grain size) in summer. However, they also discussed that their
77 sensitivities could be low as a consequence of prescribing atmospheric forcing in their model
78 setup, so parametric uncertainties are expected to be larger year round (particularly in winter) in
79 a fully-coupled model. Since we also run stand-alone CICE5 given that our aim is to demonstrate
80 the utility of parameter estimation (PE) for sea ice, we target the summer season.

81 Despite the importance of sea ice model parameters, few studies have tried to estimate or
82 reduce the parametric uncertainties, partly due to the large effort and computational cost if
83 parameter calibration is done in a trial-and-error fashion. A more systematic way is through DA.
84 *Anderson* (2001) demonstrated the feasibility of updating parameters using an ensemble filter in
85 a low-order model. *Annan et al.* (2005) was among the first to apply an ensemble filter to
86 estimate parameters in a complex earth system model. *Massonnet et al.* (2014) employed the
87 ensemble Kalman filter (EnKF) in a sea ice model to estimate three parameters that control sea
88 ice dynamics. In addition to achieving their goal of improving the sea ice drift, they also realized
89 slight improvements in the SIT distribution and extent as well as in the sea ice export through the
90 Fram Strait.

91 Our purpose is to expand upon previous studies to explore the feasibility of optimizing sea
92 ice parameters by asking how different observations (concentration and thickness in this study)
93 would constrain the parameters differently, whether we need to allow parameters to vary
94 spatially, and what are the benefits of the updated parameters both when observations are
95 available for assimilation (the DA period) and when observations are not available (the forecast
96 period).



97 Our sea ice DA framework is introduced in Section 2. Experimental design and metrics used
98 to evaluate model results are described in Section 3. We present results and discussions in
99 Section 4 and conclude in Section 5.

100

101 2. The sea ice data assimilation framework

102 We use CICE5 linked to the data assimilation research testbed (DART) (*Anderson et al.*,
103 2009) within the framework of the Community Earth System Model version 2 (CESM2)
104 (<http://www.cesm.ucar.edu/models/cesm2>). The ocean is modeled as a slab ocean and the
105 atmospheric forcing is prescribed from a DART/CAM ensemble reanalysis (*Raeder et al.*, 2010).
106 Details of this framework can be found in *Zhang et al.* (2018). We extend DART/CICE to
107 include parameter estimation in this study. During the assimilation, DART and CICE5 cycle
108 between a DA step with DART and a one-day forecast step with CICE5. The state vector sent
109 from CICE5 to DART is augmented by adding selected sea ice parameters, so that when this
110 augmented state vector is passed into the filter during the DA step, the parameters and state
111 variables are both updated in the same way. The updated state variables are then post-processed
112 (if needed) and sent with the updated parameters back to CICE5 for the next one-day forecast
113 step. Unlike state variables, the parameters are not modified during CICE5 forecast steps.

114

115 3. Experiment design and evaluation methods

116 We selected a tunable parameter in the Delta-Eddington solar radiation parameterization
117 treatment (*Briegleb and Light, 2007*), R_{snw} , to be estimated in this study. R_{snw} represents the
118 standard deviation of dry snow grain radius that controls the optical properties of snow and is
119 one of the key parameters that determine snow albedo. Instead of directly tuning snow albedo



120 that could result in inconsistencies with the rest of the parameterization scheme, tuning R_{snw}
 121 changes the inherent optical properties of snow in a self-consistent fashion (*Briegleb and Light,*
 122 2007). Increasing R_{snw} leads to smaller dry snow grain radius and larger snow albedo (*Hunke et*
 123 *al.*, 2015). The default value of R_{snw} is 1.5, which corresponds to a fresh snow grain radius of
 124 $125\mu\text{m}$ (*Holland et al.*, 2012). Many parameters in CICE5, like R_{snw} , have default values based
 125 on limited field observations. As sea ice models increase in complexity, empirical parameters
 126 will increasingly need to be calibrated objectively.

127 The configurations of conducted experiments are listed in Table 1. We begin with a free run
 128 of CICE5 without DA (hereafter FREE) with 30 ensemble members. Each ensemble member has
 129 a unique value of R_{snw} , which is constant in time and space. The ensemble of R_{snw} values were
 130 random draws from a uniform distribution spanning -2 and 2. One of the ensemble members was
 131 designated as the truth with the true value of R_{snw} . Following *Zhang et al.* (2018), synthetic
 132 observations were created by adding random noise to sea ice concentration and thickness (SIC
 133 and SIT, respectively) taken from the truth ensemble member. The noise follows a normal
 134 distribution with zero mean and a standard deviation of 15% for SIC and 40 cm for SIT. The
 135 FREE experiment does not assimilate any observations, and the R_{snw} values stay the same
 136 throughout the experimental period.

137 We then conducted two pairs of experiments to test the feasibility of estimating parameters
 138 using the Ensemble adjustment Kalman filter (EAKF) (*Anderson, 2002*), which is a deterministic
 139 ensemble square root filter. Each experiment assimilates daily SIC or SIT synthetic observations.
 140 The first pair is referred to as DAsicPEcst and DAsitPEcst, while the second is referred to as
 141 DAsicPEvar and DAsitPEvar. In each pair, the former assimilates SIC observations and the latter
 142 SIT observations. In the first pair, each ensemble member has a unique spatially-uniform R_{snw} . In



143 the second pair, we allow a separate value of R_{snw} at each horizontal grid point. The augmented
144 state has the single parameter for R_{snw} in the first pair or the two-dimensional grid of R_{snw}
145 parameters in the second pair.

146 All variables in the sea ice state vector are two-dimensional in space. The parameter R_{snw} and
147 the state variables were updated based on their correlations with neighboring observations. The
148 posterior ensemble generated by DART is always spatially varying. For the first pair of
149 experiments, we take an area-weighted average of the two-dimensional posterior to get a
150 spatially invariant R_{snw} to send back to CICE5. For the second pair of experiments, the spatially
151 varying posterior R_{snw} was sent to CICE5. In all experiments, the sea ice component was run for
152 a day to produce a new state that was augmented with the previous times posterior R_{snw} (which is
153 not prognostic in CICE5) for the next DA cycle. To increase the prior ensemble spread of R_{snw} , a
154 spatially and temporally adaptive inflation was applied to the priors of both the model states and
155 R_{snw} before they were sent to the filter (*Anderson, 2007*). The initial value, standard deviation,
156 and inflation damping value of the adaptive inflation are 1.0, 0.6, and 0.9. The localization half-
157 width is 0.01 radians (about 64 km) as discussed in *Zhang et al. (2018)*. We also reject
158 observations that are three standard deviations of the expected difference away from the
159 ensemble mean of the forecast.

160 A third pair of experiments was conducted with only state DA (no parameter estimation),
161 known as DAsic and DAsit, that assimilate daily SIC and SIT synthetic observations,
162 respectively. DAsic and DAsit have the same ensemble set of R_{snw} , which is also the initial set of
163 R_{snw} in the above PE experiments. The ensemble of R_{snw} remains fixed throughout the
164 experiment period.



165 All experiments begin on 1 April 2005 and run for 18 months. Synthetic observations are
 166 assimilated only during the first 6 months (the DA period), and the next 12 months are a pure
 167 forecast period to mimic the real-world situation when making a forecast. The values of R_{snw} are
 168 unchanged once DA ceases. We chose not to utilize DA beyond October 2005 for two reasons.
 169 First, sea ice states have small ensemble spread in winter, as illustrated in Figure 1a, so DA
 170 updates tend to be small. In contrast, the relatively larger spread from April to October ensures
 171 that assimilating observations can have more impact in updating model state variables and
 172 parameters. Second, the snow albedo feedback only influences the sea ice state when sunlight is
 173 present.

174 Several commonly used error indices were calculated to evaluate the performance of the
 175 experiments. The temporal averaged root-mean-square error ($RMSE_s$) and the area weighted
 176 spatial averaged root-mean-square error ($RMSE_t$) are defined as follows:

$$177 \quad RMSE_s = \sqrt{\frac{\sum_{i=1}^N (\overline{x_i^m} - x_i^t)^2}{N}}; \quad RMSE_t = \sqrt{\frac{\sum_{j=1}^M (\overline{x_j^m} - x_j^t)^2}{M}}$$

178 where i and j are the indices in time and space, x may refer to parameters or model states, N is
 179 the number of days and M is the number of grid cells. The superscripts m and t refer to model
 180 and truth, respectively. The overbar indicates the mean of the model ensemble.

181 Model bias is defined as the mean of the 30 member ensemble of the experiments minus the
 182 truth. Absolute bias difference (ABD) between two experiments is defined as follows:

$$ABD = \left| \overline{x_i^{case1}} - x_i^t \right| - \left| \overline{x_i^{case2}} - x_i^t \right|$$

183 where x may refer to parameters or model states, the superscripts t refers to the truth, and *case1*
 184 and *case2* refer to the two experiments to compare. The overbar indicates the mean of the model
 185 ensemble. RAB indicates how much improvement or degradation DA offers relative to the
 186 control (FREE) run.



187 4. Results and Discussion

188 4.1 Temporally and spatially invariant parameters

189 The ensemble mean of FREE underestimates SIC throughout the year (Figure 1a) partly
190 because our arbitrary ensemble member selected as the truth has an above average R_{snw} (Figure
191 1c). As such, we would intuitively expect R_{snw} to have a positive increment as a result of
192 assimilating SIC observations. Figure 1b confirms that R_{snw} increments are positive, with the
193 posterior ensemble mean gradually approaching the true value during the DA period in the
194 spatially-constant PE experiments (DAsicPEcst and DAsitPEcst). The posterior R_{snw} has smaller
195 ensemble spread than the prior R_{snw} (also see Figure S1d, e, and f), which is consistent with the
196 EAKF theory. In Figure 1c DAsitPEcst outperforms DAsicPEcst starting in June, indicating that
197 SIT provides more information than SIC for R_{snw} . Similarly, with state-only DA, *Zhang et al.*
198 (2018) found that SIT is more efficient than SIC observations at constraining state variables.
199 There could be several reasons why the rate at which R_{snw} approaches the true value decreases
200 with time. First, the ensemble spread of R_{snw} may be insufficient because no uncertainty is
201 introduced into R_{snw} in CICE5 during the forecast step. It is an open question how much
202 additional uncertainty should be introduced into the parameters. To help avoid filter divergence,
203 we apply the prior adaptive inflation to the parameters (as well as to the model states), which
204 may still be not enough. Second, the correlation between R_{snw} and the observations may be too
205 weak. Solar radiation becomes very low by the end of September and hence R_{snw} has little impact
206 on sea ice, which explains the weak correlation between R_{snw} and the observations (further
207 discussed below). Either reason could result in a negligible update to R_{snw} .

208 The correlations between R_{snw} and the observations have unique spatial patterns and evolve
209 with time. On May 1st, the correlation between R_{snw} and SIC is generally positive (Figure 2a).



210 The positive correlations are significant especially where SIC is under $\sim 100\%$. Larger R_{snw}
 211 corresponds to higher snow albedo and more reflected sunlight, which in turn delays the melting
 212 of sea ice. The correlations are still significant along the ice edges in August (Figure 2c) and
 213 become noisier and have less significant values by the end of the melt season (Figure 2e). The
 214 correlation between R_{snw} and SIT has different spatial patterns (Figures S2b, S2d, and S2f).
 215 Negative correlations between R_{snw} and SIT on May 1st can be seen in the Chukchi Sea, Beaufort
 216 Sea, and East Siberian Sea, where R_{snw} and SIC have positive correlations. This suggests that
 217 where SIC increases with R_{snw} in spring, it is possible that SIT actually decreases, which might
 218 be due to elevated concentration raising the compressive strength and reducing sea ice
 219 deformation. While a brighter surface is able to reduce thickness over large regions in spring, the
 220 effect is mostly gone by the end of summer when positive correlation prevails.

221

222 4.2 Spatially varying R_{snw}

223 We discussed in section 4.1 that processes relating R_{snw} and observed quantities have
 224 complex spatial features. The spatial map of the posterior R_{snw} and the reduction in the ensemble
 225 spread of R_{snw} after EAKF in the first pair of experiments (Figure S1) also suggest that the
 226 updates are concentrated on the ice marginal zones. It may be too crude to use a single value of
 227 R_{snw} for the whole Arctic. We let R_{snw} be a spatially varying parameter in the second pair of PE
 228 experiments, even though the true R_{snw} is spatially invariant. The spatial features of R_{snw} will
 229 purely depend on how R_{snw} correlates with the observations. As in DASicPEcst and DASitPEcst,
 230 the analysis field of R_{snw} is spatially varying, and we did a spatial averaging to get a single
 231 number for the next run. R_{snw} along the sea ice edges get updated more, while R_{snw} in the center
 232 is less influenced. But the averaging smoothed out this spatial feature. In DASicPEvar and



233 DASitPEvar, we didn't do spatial averaging at the end of each DA cycle, but let the spatially
 234 varying 2D field of R_{snw} be the R_{snw} field in the next run, so the spatial feature was carried along
 235 the simulation.

236 Figure 3 depicts the ABD of R_{snw} (defined in section 2) between different pairs of
 237 experiments at the end of the DA period. Figures 2a and 2d confirm that DASicPEcst and
 238 DASitPEcst improve the R_{snw} comparing to FREE. Figures 2b and 2e show the spatial feature of
 239 improvements or degradations in R_{snw} for the two spatially varying PE experiments. They both
 240 show the contrast between the ice marginal zones and the central Arctic. Improvements are
 241 mostly seen along the ice edges. Spotty improvements in the inner Arctic can be found in
 242 DASitPEvar (Figure 3e), while degradations are prevailing in the inner Arctic in DASicPEvar
 243 (Figure 3e). Figures 2c and 2f highlight the improvements or degradations from allowing R_{snw} to
 244 vary spatially. The general features are that DASicPEvar and DASitPEvar have reduced R_{snw}
 245 biases more along the ice edges compared with DASicPEcst and DASitPEcst. However,
 246 degradations (Figure 3c) or negligible improvements (Figure 3f) are found in the central Arctic.
 247 This suggests that spatially invariant PE generally works better for the whole pan-Arctic regions,
 248 while spatially varying PE can work well in the ice marginal zones but not in the central Arctic,
 249 especially when SIC is the only observed quantity. SIC has little variability in the central Arctic
 250 and hence assimilating the SIC observations will not add much information for parameters or
 251 model states. The degradations in R_{snw} but slight improvements in SIC (discussed in section 4.3)
 252 in the central Arctic suggest that R_{snw} is likely over adjusted to cancel out other errors (e.g., noise
 253 from atmospheric forcing fields).

254

255 4.3 Additional improvements in model states



We demonstrated that R_{snw} approaches the true value by assimilating SIC or SIT (at different rates) in the previous sections. We now investigate whether PE also improves the simulation of model states, beginning with timeseries of the pan-Arctic sea ice area and volume in all of our experiments (see Figure 4).

In our preceding work, we showed that assimilating SIC and SIT could improve model states (Zhang *et al.*, 2018), which can also be confirmed in Figure 4. During the DA period, DAsic can efficiently reduce biases in area, but DAsic has limited influence on volume. Within about a month into the forecast period, DAsic improves neither area nor volume. In contrast, DAsit is highly beneficial at reducing both area and volume during the DA period, with at least some improvement to volume persisting through the whole 1-year forecast period.

We find that updating R_{snw} has a relatively large impact on volume beginning in spring of the forecast period (Figure 4b). Either treating R_{snw} as a spatially varying or constant parameter has about the same effect until late summer of the forecast period. In fact, all of the PE experiments outperform the state-only DA experiments in the forecast period. As shown in Table 1, SIT DA with PE always performs the best, reducing the bias in area by up to 63% and reducing the bias in volume by up to 73%. SIC DA with PE is second best in terms of simulating the area, reducing the bias by up to 37%. SIC DA with PE is comparable to DAsit in simulating volume, reducing the bias by around 30%.

Finally, we compare the spatial patterns of bias reduction in SIC and SIT from PE experiments by comparing RMSE of SIT in DAsicPEcst and DAsitPEcst to their state-only DA counterparts, DAsic and DAsit (see Figure 5). The comparisons are made in two periods: the DA period (April to October 2005) and the forecast period (April to September 2006). Zhang *et al.* (2018) showed that the DAsic could only improve SIT along the sea ice edges. Figure 5a



279 demonstrates that DAsicPEcst offers some improvements in the central Arctic as well.
 280 Improvements resulted from a more accurate R_{snw} in the forecast period are more prominent
 281 (Figure 5b). For DAsitPEcst, SIT is improved almost everywhere in the Arctic, with slight
 282 degradations along the ice edges (Figure 5c). The improvements persist throughout the forecast
 283 period (Figure 5d).

284

285 5. Conclusions

286 We extend the functionality of DART/CICE to do parameter estimation (PE) through the
 287 EAKF as well as updating the model states. One of the key parameters determining sea ice
 288 surface albedo, R_{snw} , is estimated as an example in this study. R_{snw} is updated using the filter. We
 289 designed a series of perfect model observing system simulation experiments (OSSEs) to
 290 demonstrate the feasibility of PE in CICE5. Results show that R_{snw} gradually approaches the true
 291 value during the data assimilation (DA) period (from April to October 2005). Updating
 292 parameters with PE could further improve the model state estimation but not prominently in the
 293 DA period. During the forecast period, with a better representation of the parameter, the PE
 294 experiments show significant superiority over the state-only DA experiments, both in SIC and
 295 SIT. The results in the forecast period indicate that by updating parameters as well as state
 296 variables, assimilating SIC observations only is comparable to assimilating SIT observations. We
 297 concluded that SIT is the most important variable to be observed in *Zhang et al. (2018)*, but
 298 satellite observations of SIT have large uncertainties and only cover a short time period. We
 299 could alternatively improve model parameters by assimilating SIC observations with the ultimate
 300 goal of improving SIT. Results from the subset of experiments treating R_{snw} as a spatially
 301 varying parameter suggest that the R_{snw} biases are mostly reduced along the sea ice edges but not



302 as much in the central Arctic. We suggest that varying R_{snw} spatially is not effective when
303 conducting DA for the whole Arctic, but worth exploring when it comes to regional studies, such
304 as in the seasonal sea ice zones.

305

306 **Acknowledgements**

307 This work was supported by the National Oceanographic and Atmospheric Administration
308 Climate Program Office through grant NA15OAR4310161. We thank Adrian Raftery and
309 Hannah Director for helpful discussions, and David Bailey and Marika Holland for suggestions
310 about choosing the proper parameters to estimate in the Los Alamos sea ice model. We
311 acknowledge Computational & Information Systems Lab at the National Center for Atmospheric
312 Sciences and Texas Advanced Computer Center at The University of Texas at Austin for
313 providing high performance computing resources that have contributed to the research results
314 reported within the paper. The model outputs archiving is underway and will be available in the
315 figshare repository.

316

317

318

319

320

321

322

323

324



325 References

- 326 Anderson, J. (2002), An ensemble adjustment Kalman filter for data assimilation, *Mon. Weather*
 327 *Rev.*, *129*, 2884–2903.
- 328 Anderson, J. L. (2007), An adaptive covariance inflation error correction algorithm for ensemble
 329 filters, *Tellus*, *59* (2), 210–224.
- 330 Anderson, J. L., T. Hoar, K. Raeder, H. Liu, N. Collins, R. Torn, and A. Arellano (2009), The
 331 Data Assimilation Research Testbed: A community facility. *Bull. Amer. Meteor. Soc.*, *90*,
 332 1283–1296, doi:10.1175/2009BAMS2618.1.
- 333 Annan, J. D., J. C. Hargreaves, N. R. Edwards, and R. Marsh (2005), Parameter estimation in an
 334 intermediate complexity earth system model using an ensemble Kalman filter, *Ocean Model*,
 335 *8*, 135–154, doi:10.1016/j.ocemod.2003.12.004.
- 336 Blanchard-Wrigglesworth, E., K.C. Armour, C. M. Bitz, and E. deWeaver (2011), Persistence
 337 and inherent predictability of Arctic sea ice in a GCM ensemble and observations, *J. Climate*,
 338 *24*, 231–250, doi: 10.1175/2010JCLI3775.1.
- 339 Briegleb, B. P., and B. Light (2007), A Delta-Eddington multiple scattering parameterization for
 340 solar radiation in the sea ice component of the Community Climate System Model. NCAR
 341 Technical Note NCAR/TN-472+STR, doi:10.5065/D6B27S71.
- 342 Day, J.J., E. Hawins, and S. Tietsche (2014) Will Arctic sea ice thickness initialization improve
 343 seasonal forecast skill? *Geophys. Res. Lett.*, *41*, 7566–7575, doi:10.1002/2014GL061694.
- 344 Holland, M. M., D. A. Bailey, B. P. Briegleb, B. Light, and E. Hunke (2012), Improved sea ice
 345 shortwave radiation physics in CCSM4: The impact of melt ponds and aerosols on Arctic
 346 sea ice, *J. Climate*, *25*, 1413–1430, doi: 10.1175/JCLI-D-11-00078.1.



- 347 Hunke, E. C., W. H. Lipscomb, A. K. Turner, N. Jeffery, S. Elliott (2015), Los Alamos National
 348 Laboratory, Los Alamos, NM, USA, 116pp.
- 349 Jung, T., M. A. Kasper, T. Semmler, and S. Serrar (2014), Arctic influence on subseasonal
 350 midlatitude prediction, *Geophys. Res. Lett.*, *41*, 3676–3680, doi:10.1002/2014GL059961.
- 351 Kondrashov, D., C. Sun and M. Ghil (2008), Data assimilation for a coupled ocean-atmosphere
 352 model. Part II: Parameter estimation, *Mon. Weather Rev.*, *136.*, 5062–5076, doi:
 353 10.1175/2008MWR2544.1.
- 354 Koyama, T., J. Stroeve, J. Cassano, and A. Crawford (2017), Sea ice loss and Arctic cyclone
 355 activity from 1979 to 2014. *J. Clim.*, *30*, 4735–4754, doi:10.1175/JCLI-D-16-0542.1.
- 356 Light, B., T. C. Grenfell, and D. K. Perovich (2008), Transmission and absorption of solar
 357 radiation by Arctic sea ice during the melt season. *J. Geophys. Res.*, *113*, C03023,
 358 doi:10.1029/2006JC003977.
- 359 Lisæter, K., Rosanova, J. & Evensen, G. Ocean Dynamics (2003), Assimilation of ice
 360 concentration in a coupled ice–ocean model, using the ensemble Kalman filter, *Ocean Dyn.*,
 361 *53*, 368–388. doi:10.1007/s10236-003-0049-4.
- 362 Massonnet F., T. Fichefet, and H. Goosse (2015), Prospects for improved seasonal Arctic sea ice
 363 predictions from multi-variate data assimilation, *Ocean Modell.*, *28*, 16–25.
- 364 Massonnet, F., H. Goosse, T. Fichefet, and F. Counillon (2014), Calibration of
 365 sea ice dynamic parameters in an ocean-sea ice model using an ensemble Kalman filter, *J.*
 366 *Geophys. Res. Oceans*, *119*, 4168–4184, doi:10.1002/2013JC009705.
- 367 Raeder, K, J. L. Anderson, N. Collins, T. J. Hoar, J. E. Kay, P. H. Lauritzen and R. Pincus
 368 (2012), DART/CAM: an ensemble data assimilation system for CESM atmospheric models,
 369 *J. Climate*, *25*, 6304–6317.



370 Serreze, M. C. and J. Stroeve (2015), Arctic sea ice trends, variability and implications for
371 seasonal ice forecasting, *Phil. Trans. R. Soc. A* 373: 20140159.
372 <http://dx.doi.org/10.1098/rsta.2014.0159>.
373 Stroeve, J. C., V. Kattsov, A. Barrett, M. Serreze, T. Pavlova, M. Holland, and W. Meier (2012),
374 Trends in Arctic sea ice extent from CMIP5, CMIP3, and observations, 39, L16502,
375 doi:10.1029/2012GL052676.
376 Vitart, F., A. W. Robertson, and S2S Steering Group (2015), Sub-seasonal to seasonal prediction:
377 Linking weather and climate. Seamless Prediction of the Earth System: From Minutes to
378 Months, G. Brunet, S. Jones, and P. M. Ruti, Eds., WMO-1156, World Meteorological
379 Organization, 385–401.
380 Zhang, Y.-F., C. M. Bitz, J. L. Anderson, N. Collins, J. Hendricks, T. Hoar, and K. Raeder
381 (2018), Insights on sea ice data assimilation from perfect model observing system simulation
382 experiments, *J. Climate*, 5911–5926, doi: 10.1175/JCLI-D-17-0904.1.
383
384
385
386
387
388
389
390
391
392



Table 1. List of experiments with different configurations and RMSE of the total Arctic sea ice area and volume calculated over two experiment periods: DA (April to October, 2005) and forecast (April to September, 2006) for the seven experiments. All the experiments use the same localization half-width and prior inflation algorithm as stated in section 3.

Experiments	Observations assimilated	Parameter estimate	RMSE of Arctic sea ice area ($10^6 km^2$)		RMSE of Arctic sea ice volume ($10^3 km^3$)	
			DA	Forecast	DA	Forecast
FREE	None	None	0.250	0.343	0.711	1.302
DAsic	SIC	None	0.120 (-52%)	0.345 (4%)	0.583 (-18%)	1.285 (-1%)
DAsicPEcst	SIC	Spatially constant	0.114 (-55%)	0.217 (-37%)	0.520 (-27%)	0.887 (-32%)
DAsicPEvar	SIC	Spatially varying	0.123(-51%)	0.240(-30%)	0.601 (-16%)	1.130 (-13%)
DAsit	SIT	None	0.113(-55%)	0.327(-5%)	0.247 (-65%)	0.868 (-33%)
DAsitPEcst	SIT	Spatially constant	0.103 (-59%)	0.141 (-59%)	0.210 (-70%)	0.349 (-73%)
DAsitPEvar	SIT	Spatially varying	0.103 (-59%)	0.129 (-63%)	0.222 (-69%)	0.376 (-71%)



402 **Figure captions**

403 **Figure 1.** Time series of (a) the Arctic sea ice area and (b) sea ice volume from a CICE5 free run.

404 Each gray line represents one ensemble member, black line the ensemble mean, and red line the
 405 truth. Time series of (c) the parameter R_{snw} for two DA experiments. Blue line represents
 406 DAsicPEcst that assimilates SIC observations, magenta represents DAsitPEcst that assimilates
 407 SIT, and green line the experiment DA_PAR_CST. The red reference line indicates the true
 408 value of R_{snw} . Each error bar represents two standard deviations of the 30 ensemble members of
 409 R_{snw} . Error bar is shown for every five days.

410

411 **Figure 2.** Correlations between (a) R_{snw} and SIC and (b) R_{snw} and SIT for 2005-05-01, (c) R_{snw}
 412 and SIC and (d) R_{snw} and SIT for 2005-08-01, and (e) R_{snw} and SIC and (f) R_{snw} and SIT for
 413 2005-10-01. At each point, we calculate the correlation of R_{snw} and the observed quantities
 414 across the 30 ensemble members on the selected dates. The posterior states outputted from the
 415 experiments DAsicPEcst and DAsitPEcst are used for calculation.

416

417 **Figure 3.** The differences of absolute mean bias (ABD, see Eq 2) of R_{snw} between the DA
 418 experiments: (a) DAsicPEcst, (b) DAsicPEvar, (d) DAsitPEcst, and (e) DAsitPEvar and the
 419 control experiment FREE, and between the spatially-varying PE experiments and the spatially-
 420 constant PE experiments: (c) DAsicPEvar and DAsicPEcst, and (f) DAsitPEvar and DAsitPEcst.

421

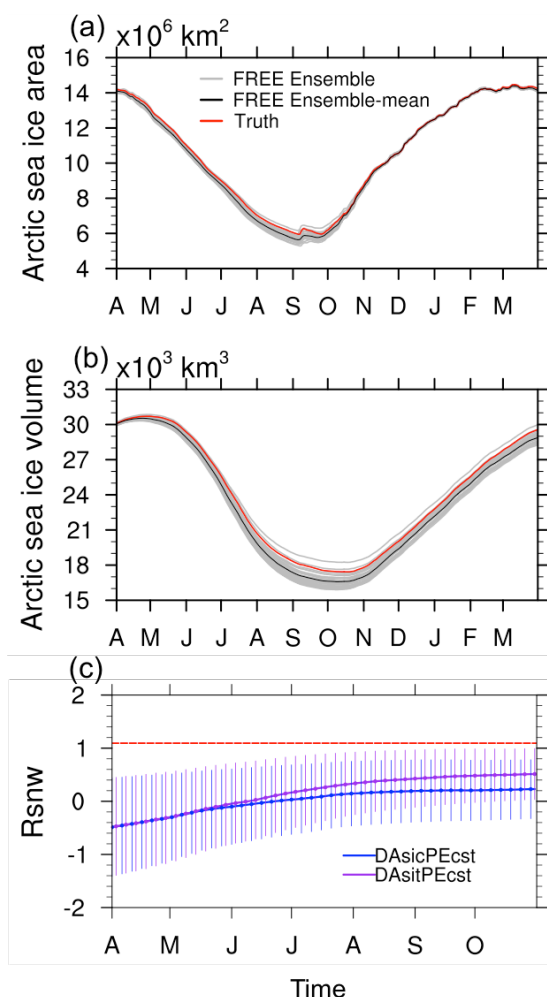
422 **Figure 4.** Daily biases of (a) the total Arctic sea ice area and (b) the total Arctic sea ice volume
 423 for FREE (black), DAsic (blue), DAsicPEcst (green), DAsicPEvar (purple), DAsit (orange),
 424 DAsitPEcst (pink), and DAsitPEvar (red). Gray dash line in each plot represents the zero



reference line. The blue line in (a) is overlapped by the purple and green lines in the first half of
 time. The black line in (a) is overlapped by the orange and blue lines in the second half of time.
 The black line in (b) is overlapped by the blue line from February to July.

Figure 5. The relative differences of RMSE of SIT between DAsicPEcst and DAsic for the (a)
 DA experiment period and (b) forecast period, and between DAsitPEcst and DAsit for the (c)
 DA experiment period and (d) forecast period. The differences of RMSE are divided by the
 RMSE of DAsic and DAsit, respectively, to get the relative differences.

Figure S1. The posterior values of Rsnw for the experiment DAsitPEcst on (a) 2005-06-01, (b)
 2005-08-01, and (c) 2005-10-01, and the differences between the ensemble spread of posterior
 Rsnw and that of prior Rsnw (the posterior minus prior) for the experiment DAsitPEcst on (d)
 2005-06-01, (e) 2005-08-01, and (f) 2005-10-01.



448

449 Figure 1. Time series of (a) the Arctic sea ice area and (b) sea ice volume from a CICE5 free

450 run. Each gray line represents one ensemble member, black line the ensemble mean, and red

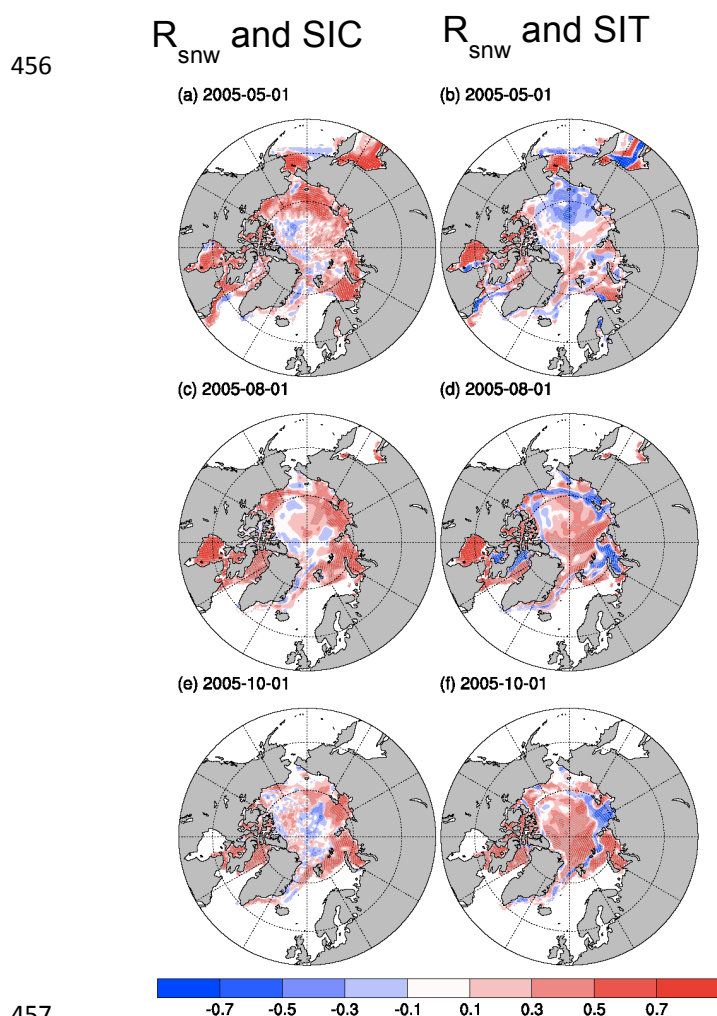
451 line the truth. Time series of (c) the parameter R_{snw} for two DA experiments. Blue line

452 represents DAsicPEcst that assimilates SIC observations, magenta represents DAsitPEcst that

453 assimilates SIT, and green line the experiment DA_PAR_CST. The red reference line

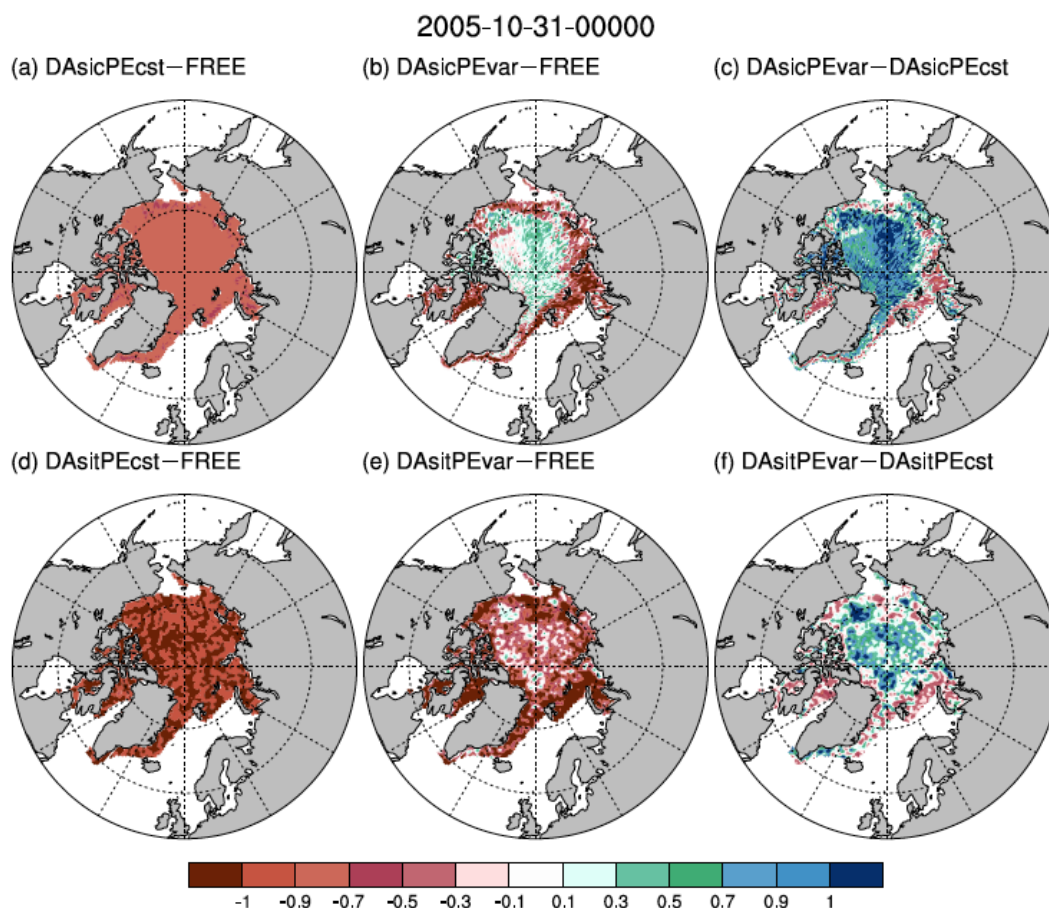
454 indicates the true value of R_{snw} . Each error bar represents two standard deviations of the 30

455 ensemble members of R_{snw} . Error bar is shown for every five days.



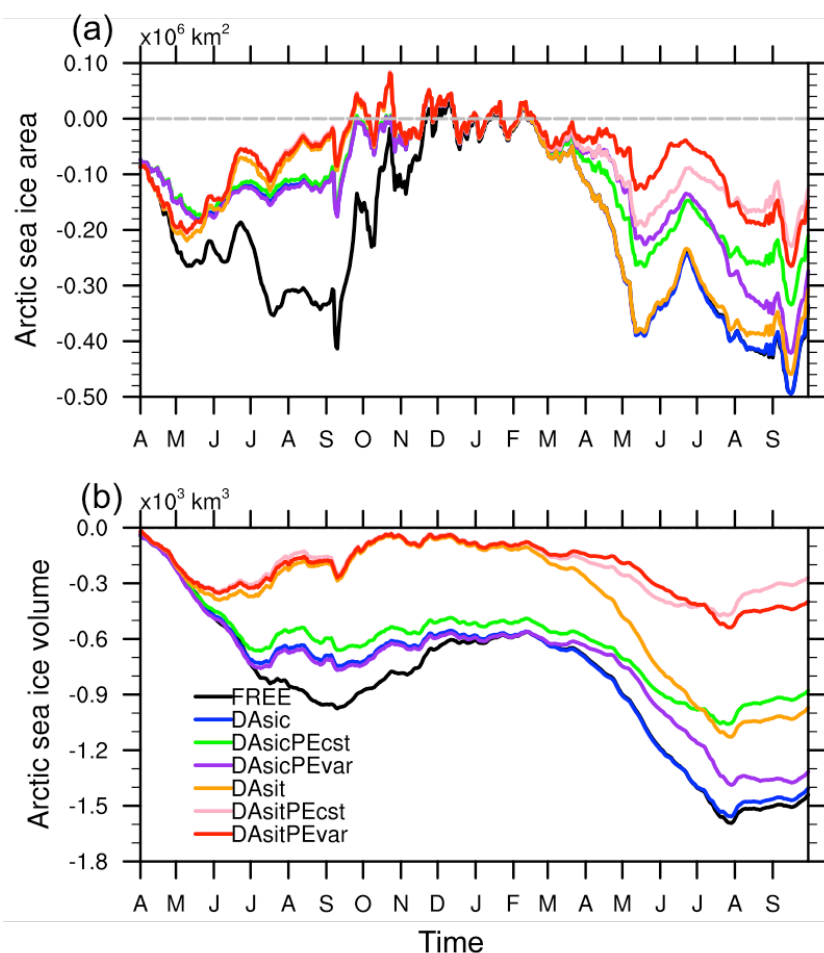
458
 459 Figure 2. Correlations between (a) R_{snw} and SIC and (b) R_{snw} and SIT for 2005-05-01, (c) R_{snw}
 460 and SIC and (d) R_{snw} and SIT for 2005-08-01, and (e) R_{snw} and SIC and (f) R_{snw} and SIT for
 461 2005-10-01. At each point, we calculate the correlation of R_{snw} and the observed quantities
 462 across the 30 ensemble members on the selected dates. The posterior states outputted from the
 463 experiments DAsicPEcst and DAsitPEcst are used for calculation.

464



465
 466
 467
 468
 469
 470
 471
 472
 473
 474
 475
 476
 477

Figure 3. The differences of absolute mean bias (ABD, see Eq 2) of R_{snw} between the DA experiments: (a) DAsicPEcst, (b) DAsicPEvar, (d) DAsitPEcst, and (e) DAsitPEvar and the control experiment FREE, and between the spatially-varying PE experiments and the spatially-constant PE experiments: (c) DAsicPEvar and DAsicPEcst, and (f) DAsitPEvar and DAsitPEcst.



478

479 Figure 4. Daily biases of (a) the total Arctic sea ice area and (b) the total Arctic sea ice volume

480 for FREE (black), DAsic (blue), DAsicPEcst (green), DAsicPEvar (purple), DAsit (orange),

481 DAsitPEcst (pink), and DAsitPEvar (red). Gray dash line in each plot represents the zero

482 reference line. The blue line in (a) is overlapped by the purple and green lines in the first half of

483 time. The black line in (a) is overlapped by the orange and blue lines in the second half of time.

484 The black line in (b) is overlapped by the blue line from February to July.

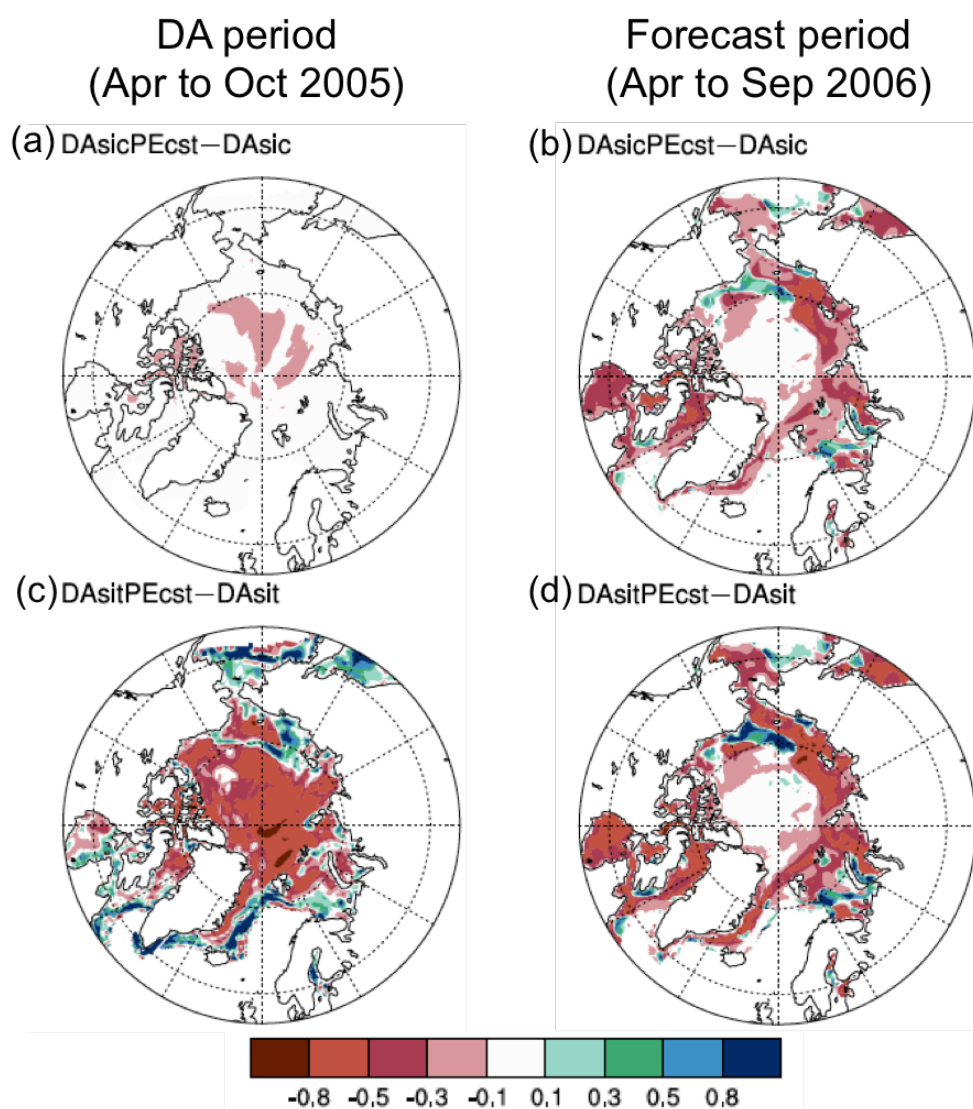
485

486

487



488



489

490

491 Figure 5. The relative differences of RMSE of SIT between $DA_{sic}PE_{cst}$ and DA_{sic} for the (a)

492 DA experiment period and (b) forecast period, and between $DA_{sit}PE_{cst}$ and DA_{sit} for the (c)

493 DA experiment period and (d) forecast period. The differences of RMSE are divided by the

494 RMSE of DA_{sic} and DA_{sit} , respectively, to get the relative differences.

495